

## Supplementary Information

### **High-Precision Measurement of Sn Isotopic Compositions in Cassiterite and Igneous Rock Reference Materials by Double Spike Technique Using MC-ICP-MS/MS**

Da-Peng Zhu, Edith Kubik, Hans Keppler, Audrey Bouvier

Universität Bayreuth, Bayerisches Geoinstitut, 95440 Bayreuth , Germany

Corresponding author

Da-peng Zhu ([Dapeng.zhu@uni-bayreuth.de](mailto:Dapeng.zhu@uni-bayreuth.de))

**Table S1: Major oxide composition (wt%) of cassiterite used in this study from the Zinnwald deposit, Germany (n = 124), determined by EMPA.**

Oxide	wt% (Mean)	2SD
SiO <sub>2</sub>	0.20	0.08
Al <sub>2</sub> O <sub>3</sub>	0.00	0.01
TiO <sub>2</sub>	0.09	0.13
WO <sub>3</sub>	0.08	0.18
MnO	0.00	0.01
CaO	1.02	0.06
Ta <sub>2</sub> O <sub>5</sub>	0.07	0.19
FeO	0.09	0.14
Nb <sub>2</sub> O <sub>5</sub>	0.19	0.31
V <sub>2</sub> O <sub>5</sub>	0.01	0.03
SnO <sub>2</sub>	98.23	0.45

**Note:** Samples were coated with a thin carbon film (~ 10 nm) prior to analysis. Measurements were performed at 15 kV accelerating voltage, 20 nA beam current, and 5 μm beam diameter. Analytical standard: SnO<sub>2</sub> (Sn), MnTiO<sub>3</sub> (Mn, Ti), Fe (Fe), Nb (Nb), Ta (Ta), Spinel (Al), Diopside (Ca, Si), W (W), and Vanadinite (V).

**Table S2: Isotope composition of the NIST SRM 3161a and calibrated double spike.**

	<sup>117</sup> Sn/ <sup>118</sup> Sn	2SD	<sup>122</sup> Sn/ <sup>118</sup> Sn	2SD	<sup>124</sup> Sn/ <sup>118</sup> Sn	2SD
			n		n	
NIST SRM 3161a	0.316684	0.000007	0.191288	0.000005	0.238950	0.000014
Double spike	11.3059	0.0013	7.49354	0.00089	0.087063	0.00002

**Table S3: Effects of double spike proportion on measured δ<sup>122</sup>Sn/<sup>118</sup>Sn of NIST 3161a.**

Double spike proportion	δ <sup>122/118</sup> Sn <sub>3161a</sub> (‰)	2 SD	n
0.4	-0.005	0.007	3
0.5	0.008	0.013	3
0.6	0.002	0.012	3

**Table S4: Recovery yields (%) of Sn during evaporation-re-dissolution and subsequent column chemistry.**

Solution	Temperature (°C)	Evaporation–re-dissolution (%)	Post-column chemistry (%)
Pure Sn	60	101.55	60.25
	80	93.25	68.86
Sn + matrix <sup>1</sup>	80	92.85	51.50
	120	68.90	59.56
ICP solution <sup>2</sup> (rep.1)	120	98.30	99.85
ICP solution <sup>2</sup> (rep.2)	120	99.85	100.9
ICP solution <sup>2</sup> (rep.3)	120	98.62	88.48
ICP solution <sup>2</sup> (rep.4)	120	90.43	91.06

<sup>1</sup> Matrix elements: Ag, Al, As, Ba, Be, Bi, Ca, Cd, Co, Cr, Cs, Cu, Fe, Ga, In, K, Li, Mg, Mn, Na, Ni, Pb, Rb, Se, Sr, Tl, U, V, Zn.

<sup>2</sup> ICP solution contains Au, Hf, Ir, Pd, Pt, Rh, Ru, Sb, Sn, and Te.

**Table S5:  $\delta^{122}\text{Sn}/^{118}\text{Sn}_{3161a}$  values and Sn recovery yields of NIST SRM 3161a after evaporation at different temperatures.**

Temperature (°C)	$\delta^{122/118}\text{Sn}_{3161a}$ (‰)	2 SD (n =3)	Recovery (%)
70	-0.003	0.023	82
90	0.002	0.017	78
110	-0.019	0.009	51
130	-0.023	0.014	56

**Table S6: Effect of concentration mismatch on  $\delta^{122}\text{Sn}/^{118}\text{Sn}_{3161a}$ .**

$\text{Sn}_{\text{sample}}/\text{Sn}_{\text{standard}}$	$\delta^{122/118}\text{Sn}_{3161a}$ (‰)	2 SE
0.6	-0.065	0.030
0.7	-0.039	0.060
0.8	-0.030	0.032
0.9	-0.012	0.027
1.0	0.000	0.030
1.1	0.044	0.035
1.2	0.026	0.031
1.3	0.053	0.027
1.4	0.065	0.033

**Table S7: Long-term reproducibility of Sn isotope measurements.**

NIST 3161a						ICP-MS Sn solution	
No.	$\delta^{122/118}\text{Sn}_{3161}$ a (‰)	No.	$\delta^{122/118}\text{Sn}_{3161}$ a (‰)	No.	$\delta^{122/118}\text{Sn}_{3161}$ a (‰)	No.	$\delta^{122/118}\text{Sn}_{3161}$ a (‰)
1	-0.008	26	0.003	51	-0.007	1	0.178
2	-0.002	27	-0.003	52	0.002	2	0.187
3	0.000	28	-0.016	53	-0.003	3	0.186
4	0.001	29	-0.006	54	0.021	4	0.198
5	0.017	30	-0.006	55	0.002	5	0.150
6	0.012	31	-0.002	56	0.004	6	0.157
7	0.009	32	-0.015	57	0.025	7	0.195
8	-0.001	33	-0.031	58	0.019	8	0.197
9	-0.001	34	0.000	59	0.005	9	0.156
10	-0.003	35	-0.002	60	0.004	10	0.191
11	0.005	36	0.013	61	0.010	11	0.177
12	0.002	37	-0.005	62	0.010	12	0.171
13	0.003	38	-0.004	63	0.005	13	0.186
14	0.003	39	-0.005	64	0.011	14	0.184
15	0.003	40	0.006	65	0.009	15	0.184
16	-0.003	41	-0.003	66	-0.001	16	0.170
17	-0.008	42	0.006	67	0.009	17	0.190
18	0.000	43	0.009	68	-0.009	18	0.191
19	-0.002	44	0.007	69	0.011	19	0.154
20	-0.002	45	0.009	70	0.010	20	0.173
21	-0.004	46	0.008	71	0.002	21	0.175
22	0.004	47	-0.009			22	0.148
23	0.001	48	-0.003				
24	0.003	49	-0.009				
25	0.003	50	-0.003				



Figure S1. Experimental dissolution of cassiterite in NaOH conducted within different container materials. (a) Outer Pt crucibles containing inner MgO (left) and Al oxide (right) crucibles inside the muffle furnace; (b) powdery reaction products observed in the MgO crucible; (c) products adhering to the bottom of the Al oxide crucible.

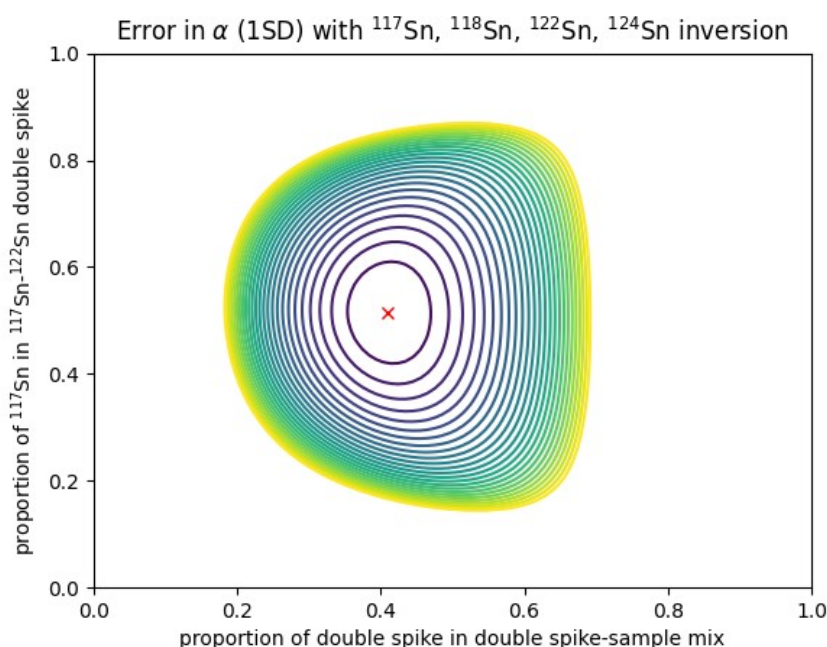


Figure S2. A contour plot illustrates the propagation of uncertainties on the natural fractionation factor  $\alpha$  (1SD) for the  $^{117}\text{Sn}$ ,  $^{118}\text{Sn}$ ,  $^{122}\text{Sn}$ , and  $^{124}\text{Sn}$  inversion. The diagram explores how the error varies as a function of both the proportion of double spike added to the sample mixture and the relative contribution of  $^{117}\text{Sn}$  in the  $^{117}\text{Sn}$ - $^{122}\text{Sn}$  double spike, based on calculations with the Double Spike Toolbox. The optimal configuration, indicated by red cross, corresponds to  $\sim 40\%$  double spike in the spike-sample mixture. Contours denote increments of 1% in the error relative to the minimum value.

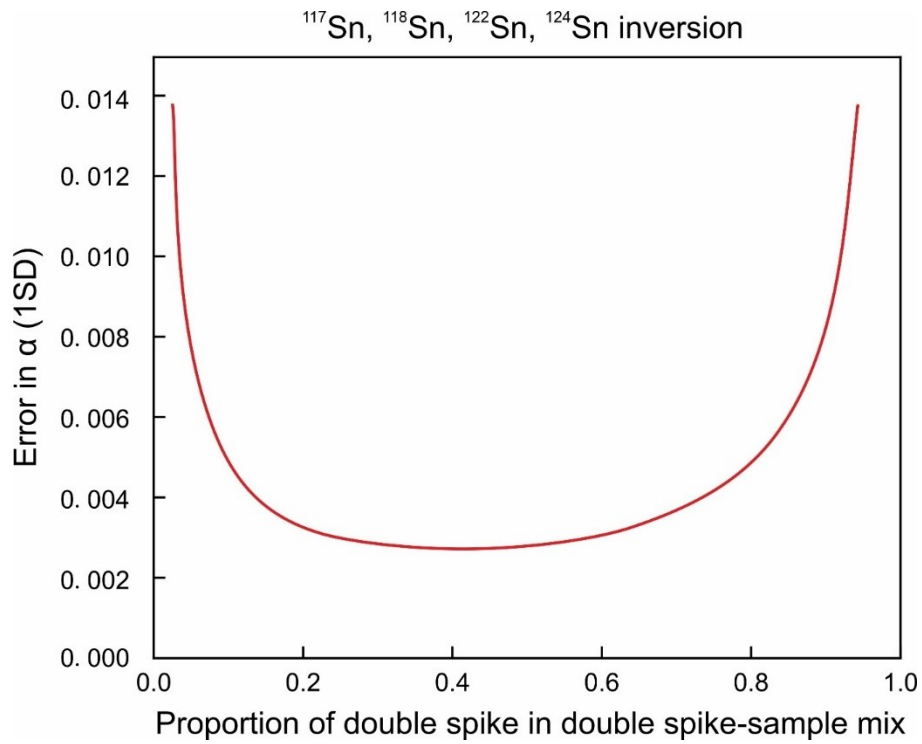


Figure S3. Optimization and validation of the <sup>117</sup>Sn-<sup>122</sup>Sn double spike. Predicted error in  $\alpha$  (1 SD) as a function of the proportion of double spike in the double spike-sample mixture, calculated for the inversion of <sup>117</sup>Sn, <sup>118</sup>Sn, <sup>122</sup>Sn, and <sup>124</sup>Sn.